

Stability Improvements at FLUTE (Verbesserung der Stabilität von FLUTE)

Master thesis
of

Marvin-Dennis Noll

at the Institute for Beam Physics and Technology

Reviewer:	Prof. Dr.-Ing. John Jelonnek
Second Reviewer:	Prof. Dr.-Ing. Thomas Zwick
Advisor:	Dr. Nigel Smale

15.11.2020 – 17.05.2021

Erklärung zur Selbstständigkeit

Ich versichere wahrheitsgemäß, die Arbeit selbstständig angefertigt, alle benutzten Hilfsmittel vollständig und genau angegeben und alles kenntlich gemacht zu haben, was aus Arbeiten anderer unverändert oder mit Abänderungen entnommen wurde und dass ich die Satzung des KIT zur Sicherung guter wissenschaftlicher Praxis in der gültigen Fassung vom 24.05.2018 beachtet habe.

Karlsruhe, den 17.05.2021, _____
Marvin-Dennis Noll

Als Prüfungsexemplar genehmigt von

Karlsruhe, den 17.05.2021, _____
Prof. Dr.-Ing. John Jelonnek

Contents

1. Introduction	3
1.1. FLUTE - Ferninfrarot Linac- und Test-Experiment	3
2. Theoretical Background	5
2.1. Linear accelerators	5
2.1.1. RF cavities	5
2.2. Relevant controlled systems theory	5
3. Problem and Previous Work	7
3.1. Problem statement	7
3.2. Previous work	7
3.2.1. 50Hz noise	7
3.2.2. Stabilizing water temperature	7
4. Own Work	9
4.1. General improvement ideas	9
4.2. Preliminary tests	9
4.3. Sensors: Selection and Evaluation	9
4.3.1. Faraday cup	9
4.3.2. PT2500 temperature sensor	9
4.4. Actuators: Selection and Evaluation	9
4.4.1. RF attenuator	9
4.4.2. Requirements	9
4.5. Overview of the device	9
4.5.1. Measurement setup	11
4.5.2. Choosing an operating point	12
4.5.3. Stability requirements and measurement of the actual stability of $V_{control}$	14
4.5.3.1. Required stability	14
4.5.3.2. Actual stability - long term	14
4.5.3.3. Actual stability - short term	15
4.5.4. Conclusion	15
4.5.5. Stability requirements and measurement of the actual stability of V_+	17
4.5.5.1. Required stability	17
4.5.5.2. Actual stability - long term	18
4.5.5.3. Actual stability - short term	19
4.5.5.4. Conclusion	21
4.5.6. Stability requirements of the case temperature θ_{case}	21
4.5.6.1. Required stability	21
4.5.6.2. Conclusion	23
4.5.7. $V_{control}$ Frequency response	24
4.5.8. Influence of RF frequency variations	25

4.5.9. Testing the Attenuator in the RF cabinet at FLUTE	25
4.6. Implementing control algorithm	26
5. Results	27
6. Conclusion and Outlook	29
6.1. Conclusion	29
6.2. Outlook	29
Appendix	31
A. Lab Test and Measurement Equipment	31
A.1. Benchtop multimeters	31
A.1.1. Agilent 34411A	31
A.1.2. Keysight 34470A	31
A.2. Data Acquisition/Switch Unit	32
A.2.1. Keysight 34972A	32
A.3. Oscilloscopes	32
A.3.1. Tektronix MSO64	32
A.4. RF signal generator	32
A.4.1. Rohde and Schwarz SMC100A	32
A.5. RF power meter	33
A.5.1. HP E4419B	33
A.6. Vector Network Analyzer	33
A.6.1. Agilent E5071C	33
A.7. Phase noise analyzer	33
A.7.1. Holzworth HA7062C	33

List of Figures

4.1. Device attenuation vs. RF frequency over DC control voltage; measured with network analyzer (see A.6.1, parameters: $\#AVG$: 16, $IF-BW$: 10 kHz)	10
4.2. Measurement setup: DUT(red), RF generator/power splitter/meter(blue), DC sources/meters(green), temperature probe(yellow)	12
4.3. Attenuation over control voltage	13
4.4. Attenuation over control voltage (zoomed in version of Figure 4.3)	13
4.5. Long term stability of $V_{control}$ as delivered by the Keysight 34972A DAC (ch. 205); measured with Keysight 34470A; room temperature during measurement: $\mu_{\vartheta} = 19.12^{\circ}\text{C}$, $\sigma_{\vartheta} = 0.28^{\circ}\text{C}$	15
4.6. Short term stability of $V_{control}$ as delivered by the Keysight 34972A DAC (ch. 205); measured with Tektronix MSO64	16
4.7. Power spectrum of $V_{control}$	16
4.8. Influence of the supply voltage on the attenuation	18
4.9. Long term stability of $V+$ as delivered by the Keysight 34972A DAC (ch. 204); measured with Keysight 34470A; room temperature during measurement: $\mu_{\vartheta} = 19.12^{\circ}\text{C}$, $\sigma_{\vartheta} = 0.28^{\circ}\text{C}$	19
4.10. Short term stability of $V+$ as delivered by the Keysight 34972A DAC (ch. 204); measured with Tektronix MSO64	20
4.11. Power spectrum of $V+$	20
4.12. Attenuation over case temperature; color scale shows time progress of the total measurement	22
4.13. Attenuation over case temperature	22
4.14. Spectrum (measured with Holzworth HA7062A (subsubsection A.7.1)) showing the effect of modulating $V_{control}$ with different frequencies (Modulation amplitude: 1 V)	24
4.15. Attenuation vs. offset frequency $f_o = f - 3\text{ GHz}$	25
4.16. Temperature of the attenuator inside the RF cabinet without a load	26

List of Tables

4.1. Requirements against the attenuator is evaluated	9
A.1. Agilent 34411A specifications	31
A.2. Agilent 34411A some SCPI commands	31
A.3. Keysight 34470A specifications	31

A.4. Keysight 34470A some SCPI commands	31
A.5. Keysight 34972A specifications	32
A.6. Keysight 34972A some SCPI commands	32
A.7. Tektronix MSO64 specifications	32
A.8. Tektronix MSO64 some SCPI commands	32
A.9. Rohde and Schwarz SMC100A specifications	32
A.10.Rohde and Schwarz SMC100A some SCPI commands	33
A.11.HP E4419B specifications	33
A.12.HP E4419B some SCPI commands	33
A.13.Agilent E5071C specifications	33
A.14.Holzworth HA7062C specifications	33

Abstract

The **F**erninfrarot **L**inac- **U**nd **T**est-**E**xperiment (FLUTE), a compact linear accelerator, is currently designed and under commission at the Karlsruhe Institute of Technology (KIT). Its main purposes are to serve as a technology platform for accelerator research, the generation of strong and ultra short THz pulses and in the future as an injection device for compact **S**torage ring for **A**ccelerator **R**esearch and **T**echnology (cSTART).

At the current commissioning state, the klystron which powers the electron gun/RF cavity and in later stages the linear accelerator is fed by a pulse forming network, which is driven by a high voltage source connected to mains power. For high and a stable output power of the cavity resonator, several parameters have to be tuned to the correct values and kept inside of sometimes small tolerance bands.

In the past, the coolant temperature of the cavities water cooling system and the dependency of the pulse forming network output of the mains voltage phase were predominant sources of instability. After dealing with these issues, the cavity output power stability was improved significantly but further improvements to the stability were still desired.

In this work instead of passively optimizing the stability of system parameters, an active approach is evaluated. By controlling the amplitude of the RF input signal of klystron, which is easily possible since it is low power, the effects of noise and/or drifts are mitigated. Here it is evaluated if a simple of the shelf voltage controllable attenuator is a feasible choice to control the RF input signal, which input data should be used and which algorithm and/or control system is suitable to determine the needed attenuator setting to stabilize RF output (of the cavity).

Furthermore since the next stage in the system depends on a stable electron bunch charge rather than cavity power, it is determined whether the charge measurements of a Faraday cup can be used to directly control electron bunch charge.

Kurzfassung

–TODO–

1. Introduction

1.1. FLUTE - Ferninfrarot Linac- und Test-Experiment

2. Theoretical Background

2.1. Linear accelerators

2.1.1. RF cavities

2.2. Relevant controlled systems theory

3. Problem and Previous Work

3.1. Problem statement

3.2. Previous work

3.2.1. 50Hz noise

3.2.2. Stabilizing water temperature

4. Own Work

4.1. General improvement ideas

4.2. Preliminary tests

4.3. Sensors: Selection and Evaluation

4.3.1. Faraday cup

The faraday cup FARC-04[1] (by RadiaBeam Technologies) is used to measure the charge of an electron bunch.

At the moment it is read out with a PCB 421A25[2] charge amplifier.

4.3.2. PT2500 temperature sensor

4.4. Actuators: Selection and Evaluation

4.4.1. RF attenuator

A RF attenuator provides a fast and simple way of influencing the RF control loop without interfering too much with existing subsystems, such as the LLRF crate from DESY.

4.4.2. Requirements

In order for the attenuator to be useful for its application, some requirements are formulated first (Table 4.1).

Table 4.1.: Requirements against the attenuator is evaluated

Requirement	Value
attenuation set point resolution	0.1 dB
attenuation repeatability	0.01 dB
temperature range	TODO
voltage supply range	TODO

4.5. Overview of the device

The ZX73-2500-S+ is a voltage controllable RF attenuator with coaxial SMA connectors by Mini-Circuits. Internally it is based on the Mini Circuits RVA-2500+, a variable SMD attenuator in the DV874 case form factor. According to equivalent circuit in the data sheet in [3] it can be assumed it is based on the common quad- π pin diode design[4].

To get a first impression of the device capabilities, the attenuation over frequency measurements from the data sheet are repeated but with a higher maximum frequency of 4 GHz

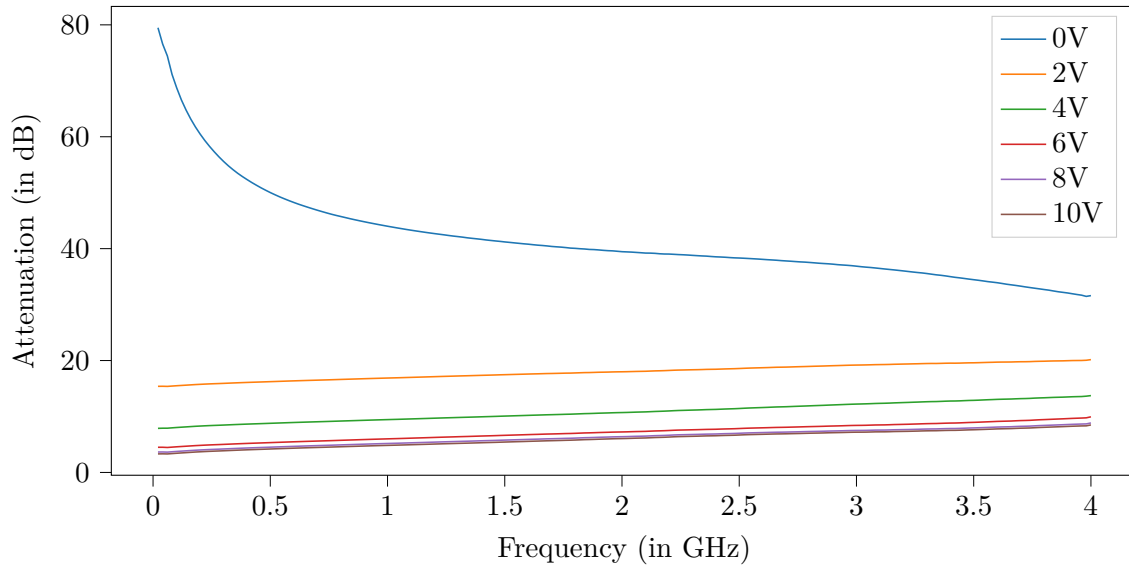


Figure 4.1.: Device attenuation vs. RF frequency over DC control voltage; measured with network analyzer (see A.6.1, parameters: $\#AVG$: 16, $IF-BW$: 10 kHz)

instead of 2.5 GHz (the highest frequency for which the attenuator is specified). Figure 4.1 shows the result.

In the next sections an operating point is chosen (only relative changes in attenuation are relevant) and then the influences of environment changes on the attenuation are examined.

4.5.1. Measurement setup

For all the following sections in this chapter, common measurement setup is needed. It needs to

- supply the attenuator with the supply voltage $V+$ ¹
- feed in the (tunable) control voltage $V_{control}$
- supply RF power
- measure the attenuation
- keep track of $V+$, $V_{control}$ and the temperature ϑ_{case}

To achieve this, the setup in Figure 4.2 is used. In addition to the shown connection, each device is connected via Ethernet to a network switch and subsequently to a computer which runs a custom python program. Since all lab devices used are VXI11 compatible, they are easy to remote control. So for most measurements needed in this chapter no manual operation of the devices is needed and the program can set all parameters according to the test protocol before doing a measurement.

With the setup, a measurement frequency of about 0.5 Hz to 1 Hz can be achieved².

¹To experiment with the influence of the supply voltage on attenuation, this also should be tunable.

²Limited by the long measurement times of the HP E4419B

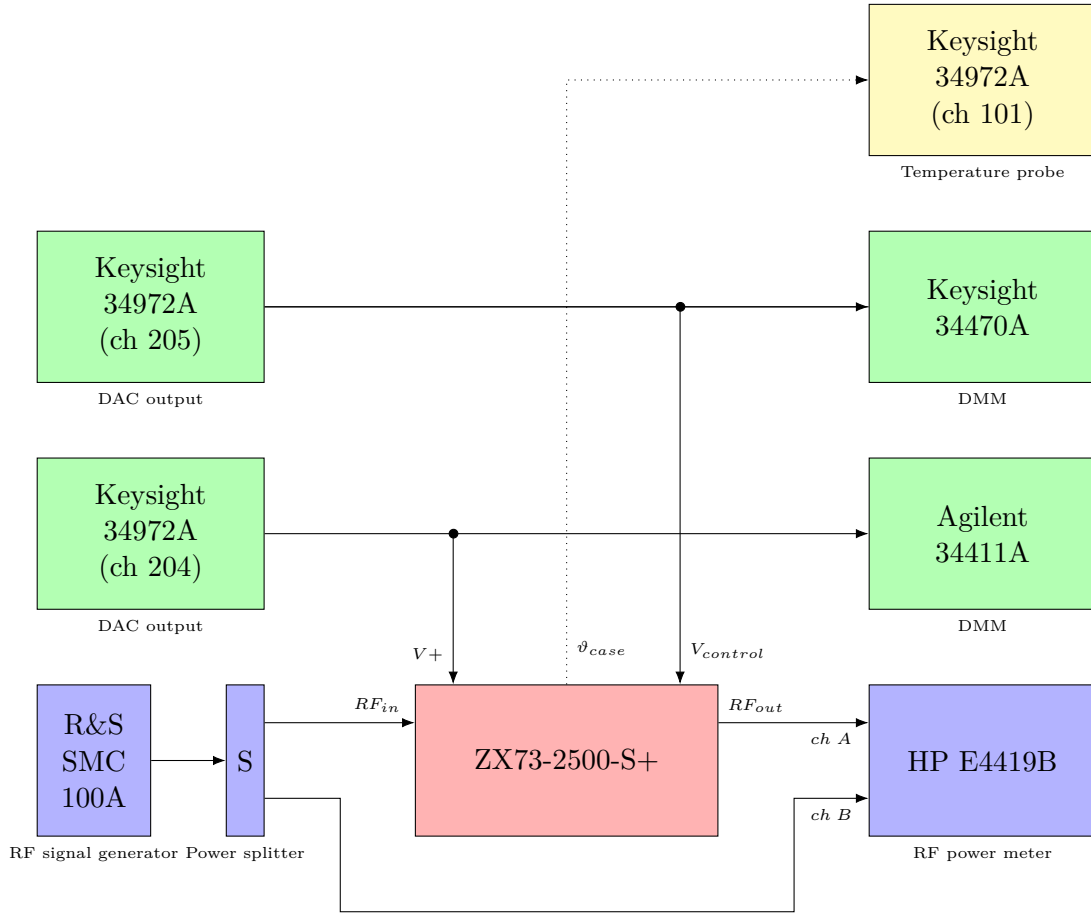


Figure 4.2.: Measurement setup: DUT(red), RF generator/power splitter/meter(blue), DC sources/meters(green), temperature probe(yellow)

4.5.2. Choosing an operating point

The spectra in Figure 4.1 already suggest that there is a nonlinear relation between the control voltage and the attenuation. This also implies a non-constant sensitivity. Therefore if a precise relative change in attenuation is desired, the needed change in the control voltage is not the same over the whole range of possible control voltages. Since the expected changes in attenuation (a few 0.1 dB) are small compared to the whole dynamic range of the device of about 80 dB, only small changes in the control voltage $V_{control}$ are necessary.

For the whole attenuator setup to meet the requirements in Table 4.1, the minimum changes in the control voltage needed by the devices operating point, need to be larger than any noise and instability of the control voltage source.

In Figure 4.3 the relation between attenuation A and the control voltage $V_{control}$ at a fixed RF frequency of 3 GHz is plotted. In addition, on the secondary axis, the sensitivity, with

$$\text{Sensitivity} := \frac{dA(V_{control})}{dV_{control}} \quad (4.1)$$

is plotted, too.

The figure shows, that for low control voltages both the absolute attenuation is quite large and the magnitude of the sensitivity is also high. Operating the attenuator in this region would require a very stable control voltage (for example at $V_{control} = 2 \text{ V}$, the sensitivity is $-10 \frac{\text{dB}}{\text{V}}$).

In Figure 4.4, the range $V_{control} = 10 \text{ V} \pm 1 \text{ V}$ is examined further. 10 V is chosen because the monotonically decreasing magnitude of the sensitivity suggests a high value but the

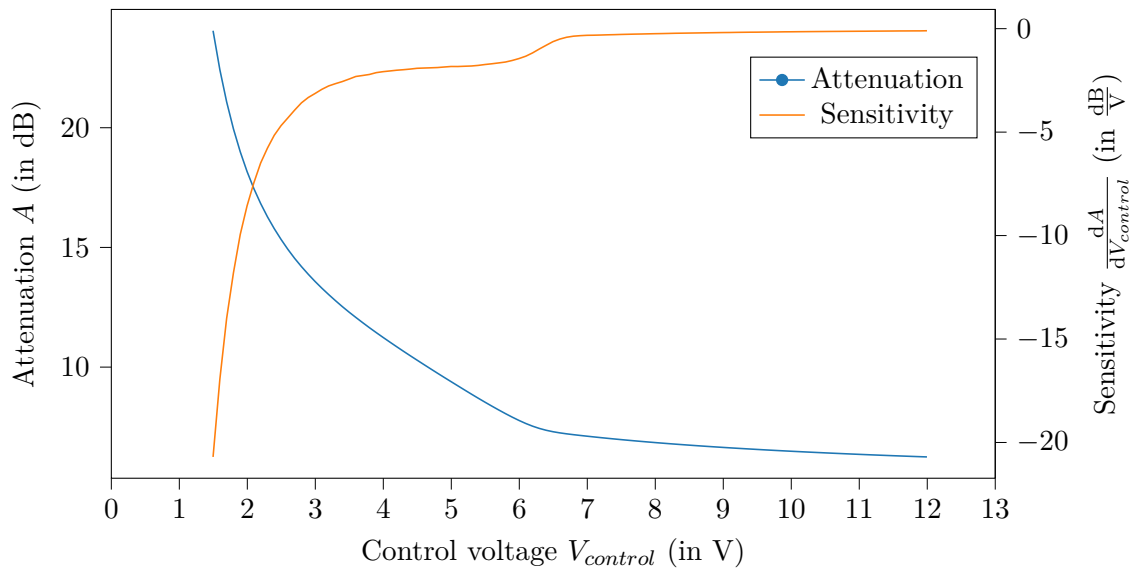


Figure 4.3.: Attenuation over control voltage

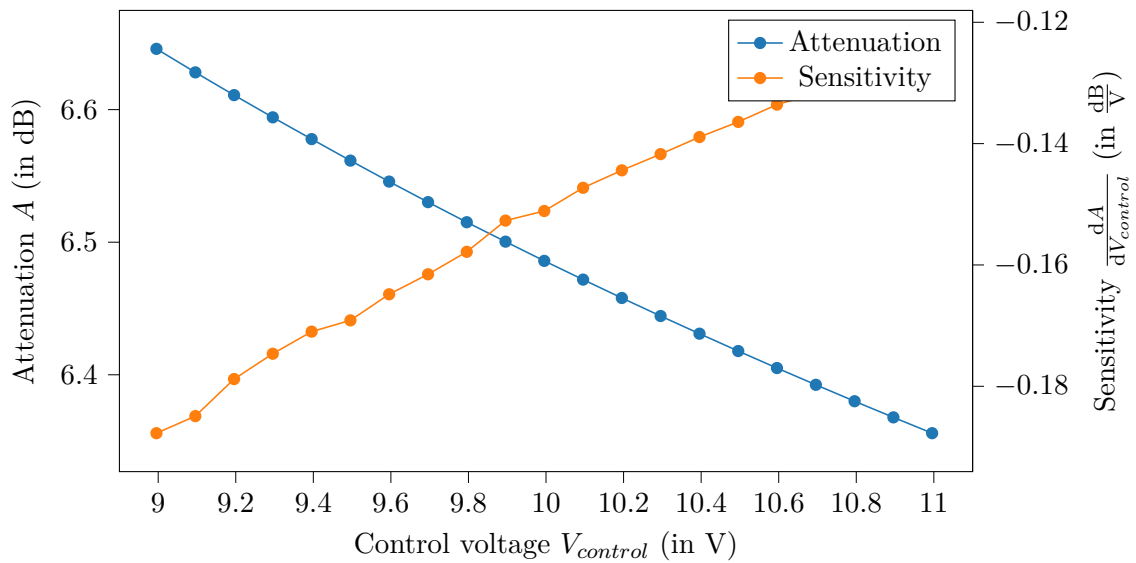


Figure 4.4.: Attenuation over control voltage (zoomed in version of Figure 4.3)

maximum output voltage of the Keysight 34972A DAC of 12 V limits the choice. With 10 V there is still a margin for further experiments.

For now, the operating point is set to $V_{control} = 10$ V. For this control voltage, the absolute attenuation is $A = 6.48$ dB and the sensitivity is $-0.1511 \frac{\text{dB}}{\text{V}}$.

4.5.3. Stability requirements and measurement of the actual stability of $V_{control}$

4.5.3.1. Required stability

Figure 4.4 shows the attenuation A to be almost linearly dependent of $V_{control}$ in the vicinity of the operating point $V_{control,o} = 10\text{ V}$, thus the function $A(V_{control})$ can be approximated by its first order derivative around $V_{control,o}$:

$$A(V_{control}) - A(V_{control,o}) = \left. \frac{dA(V_{control})}{dV_{control}} \right|_o \cdot (V_{control} - V_{control,o}) \quad (4.2)$$

$$\Delta A(V_{control}) = \left. \frac{dA(V_{control})}{dV_{control}} \right|_o \cdot \Delta V_{control} \quad (4.3)$$

With $\left. \frac{dA(V_{control})}{dV_{control}} \right|_o = -0.1511 \frac{\text{dB}}{\text{V}}$ and the required $\Delta A < 0.01\text{ dB}$ (so $\Delta A < 0.005\text{ dB}$ in one direction), the allowed deviation of $V_{control}$ from $V_{control,o}$, i.e. $\Delta V_{control}$ becomes

$$|\Delta V_{control}| = |\Delta A(V_{control})| \cdot \left| \left[\left. \frac{dA(V_{control})}{dV_{control}} \right|_o \right]^{-1} \right| \quad (4.4)$$

$$= 0.005\text{ dB} \cdot 6.618 \frac{\text{V}}{\text{dB}} = 33.09\text{ mV} \quad (4.5)$$

Equation 4.4 requires the control voltage to be stable in the interval of $\pm 33\text{ mV}$ around the operating point.

4.5.3.2. Actual stability - long term

To assess the actual stability of $V_{control}$, delivered from the Keysight 34972A (see subsection A.2.1) DAC, first its long term stability over the course of one day is measured. For that the voltage is taken once every 2 seconds with a Keysight 34470A multimeter (see subsection A.1.2). The result is shown in Figure 4.5.

This measurement shows the stability of $V_{control}$ to be

$$\sigma_{V_{control},longterm} = 0.173\text{ mV} \quad (4.6)$$

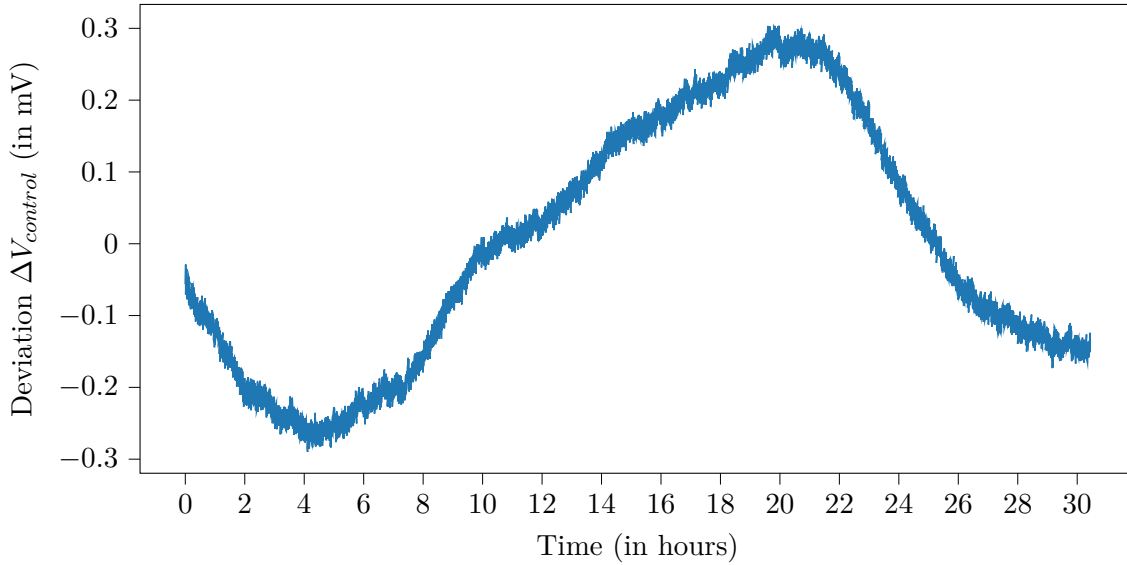


Figure 4.5.: Long term stability of $V_{control}$ as delivered by the Keysight 34972A DAC (ch. 205); measured with Keysight 34470A;
room temperature during measurement: $\mu_{\vartheta} = 19.12^{\circ}\text{C}$, $\sigma_{\vartheta} = 0.28^{\circ}\text{C}$

4.5.3.3. Actual stability - short term

Since the Keysight 34470A has a limited bandwidth of 15 kHz, higher frequency noise is not captured in Figure 4.5. Therefore for short term stability the DAC channel is measured again with a Tektronix MSO64 oscilloscope (subsubsection A.3.1, on the 500 MHz bandwidth setting). The resulting time signal is shown in Figure 4.6, the spectrum shows Figure 4.7.

This measurement shows the stability of $V_{control}$ to be

$$\sigma_{V,control,shortterm} = 7 \text{ mV} \quad (4.7)$$

4.5.4. Conclusion

With an allowed deviation of 33 mV, the output resolution of the Keysight 34972A DAC ($24\text{V}/2^{16}-1 = 366.22\text{ }\mu\text{V}$) and its stability (0.173 mV long term, 7 mV short term) pose no problems on the device operation (if the other parameters are to be assumed with no error).

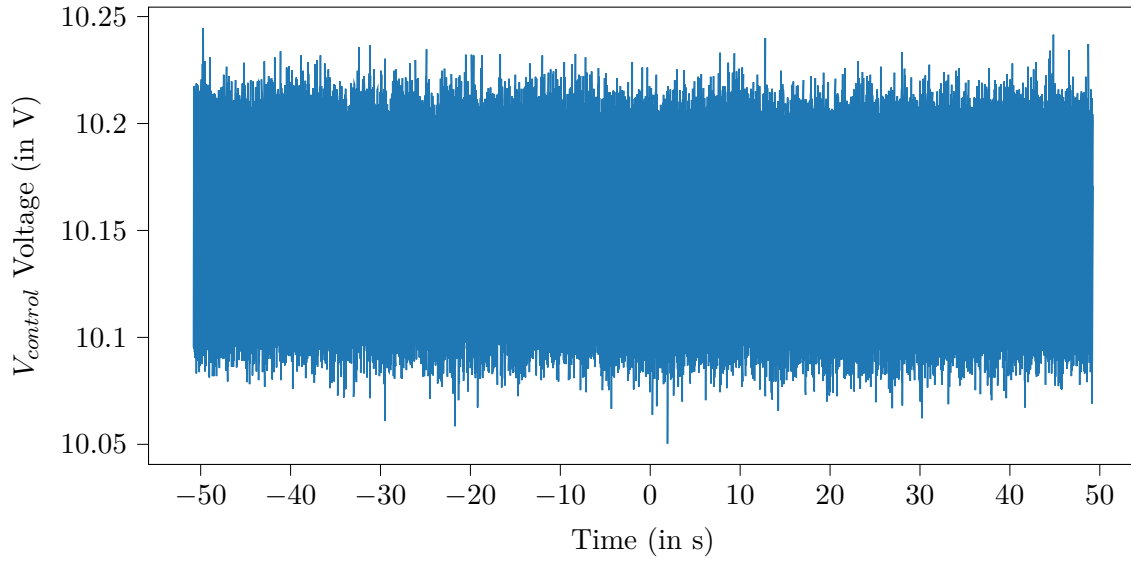


Figure 4.6.: Short term stability of $V_{control}$ as delivered by the Keysight 34972A DAC (ch. 205); measured with Tektronix MSO64

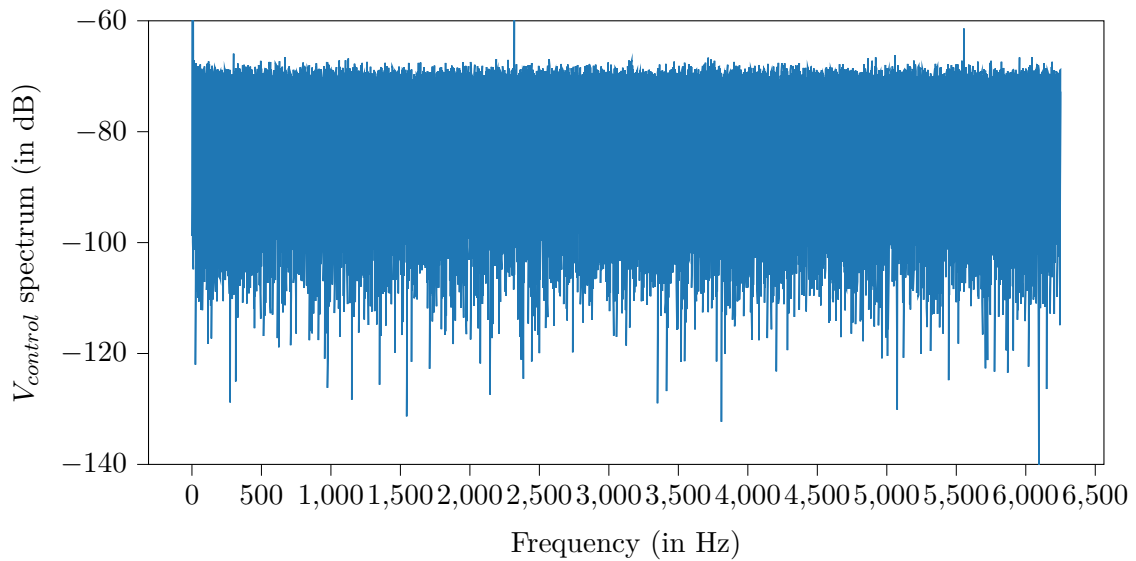


Figure 4.7.: Power spectrum of $V_{control}$

4.5.5. Stability requirements and measurement of the actual stability of V_+

4.5.5.1. Required stability

To get the required stability for the power supply voltage, the effect of the power supply voltage V_+ on the attenuation has to be examined first. For that V_+ is varied $\pm 0.2 \text{ V}$ around the nominal supply voltage of $V_{+0} = 3 \text{ V}$, all other parameters are kept constant and the attenuation is measured. To make the measurement more robust against fluctuations of the room temperature and drift of the devices, the procedure of stepping through the voltages is repeated and the means for each set V_+ are computed. The result is shown in Figure 4.8.

This leads to:

$$\Delta A(V_+) = \left. \frac{dA(V_+)}{dV_+} \right|_o \cdot \Delta V_+ \quad (4.8)$$

$$\Delta A(V_+) = 0.00375 \frac{\text{dB}}{\text{V}} \cdot \Delta V_+ \quad (4.9)$$

which means the allowed deviation of V_+ from V_{+0} becomes

$$|\Delta V_+| = |\Delta A(V_+)| \cdot \left| \left[\left. \frac{dA(V_+)}{dV_+} \right|_o \right]^{-1} \right| \quad (4.10)$$

$$= 0.005 \text{ dB} \cdot 266.67 \frac{\text{V}}{\text{dB}} = 1.33 \text{ V} \quad (4.11)$$

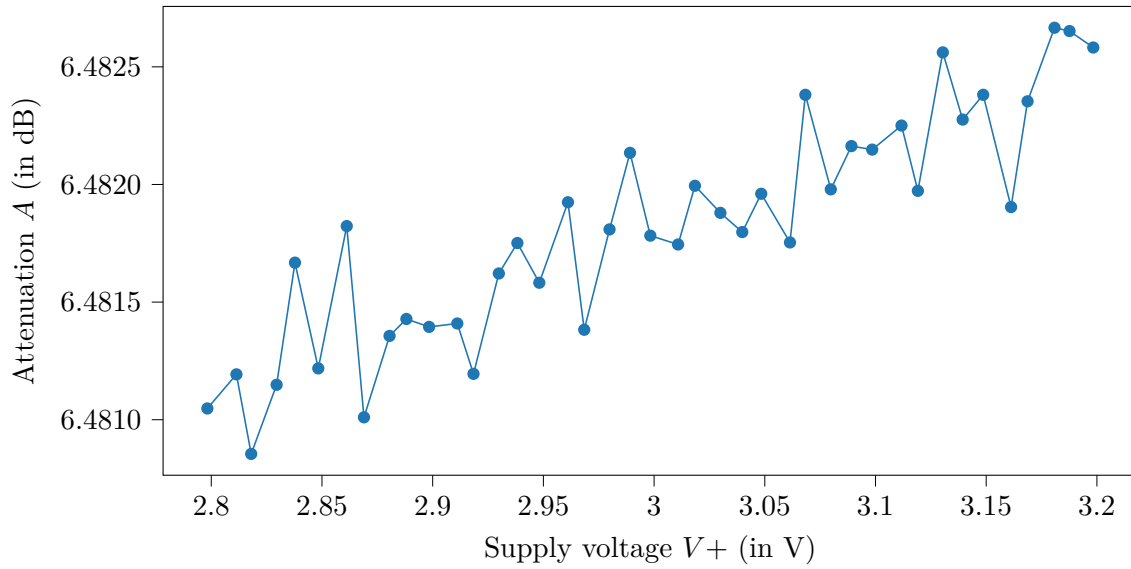


Figure 4.8.: Influence of the supply voltage on the attenuation

4.5.5.2. Actual stability - long term

This long term measurement yields a standard deviation of

$$\sigma_{V_+, longterm} = 0.154 \text{ mV} \quad (4.12)$$

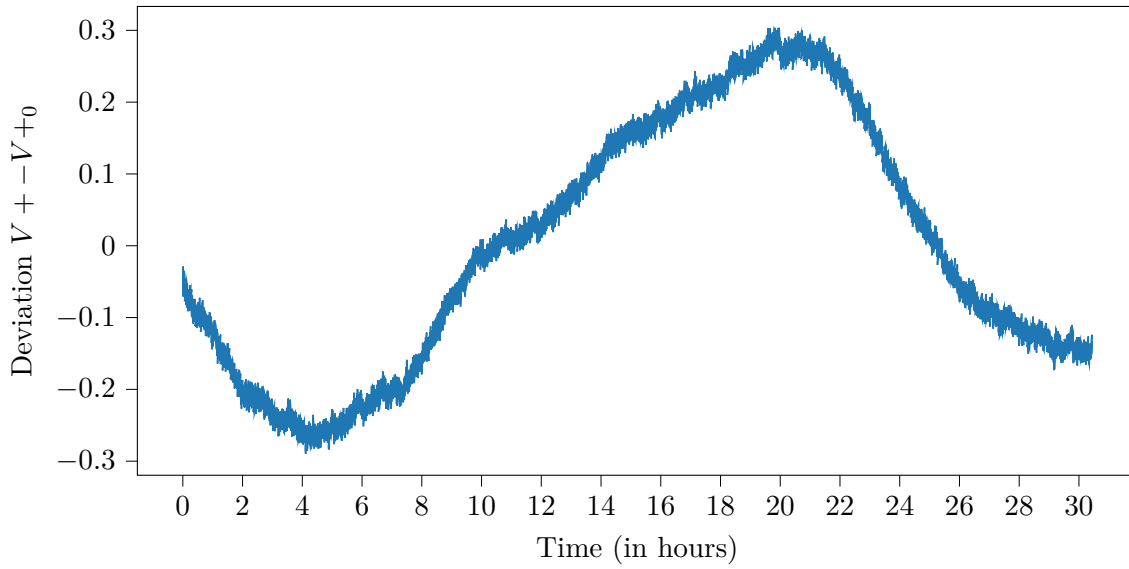


Figure 4.9.: Long term stability of $V+$ as delivered by the Keysight 34972A DAC (ch. 204); measured with Keysight 34470A;
room temperature during measurement: $\mu_{\vartheta} = 19.12^{\circ}\text{C}$, $\sigma_{\vartheta} = 0.28^{\circ}\text{C}$

4.5.5.3. Actual stability - short term

Again because of the lower bandwidth of the multimeter compared with an oscilloscope (compare subsection 4.5.3.3), the short term stability is evaluated with an oscilloscope measurement (see Figure 4.10 and Figure 4.11).

The oscilloscope measurement shows a much higher standard deviation than the multimeter measurement of

$$\sigma_{V+,shortterm} = 50 \text{ mV} \quad (4.13)$$

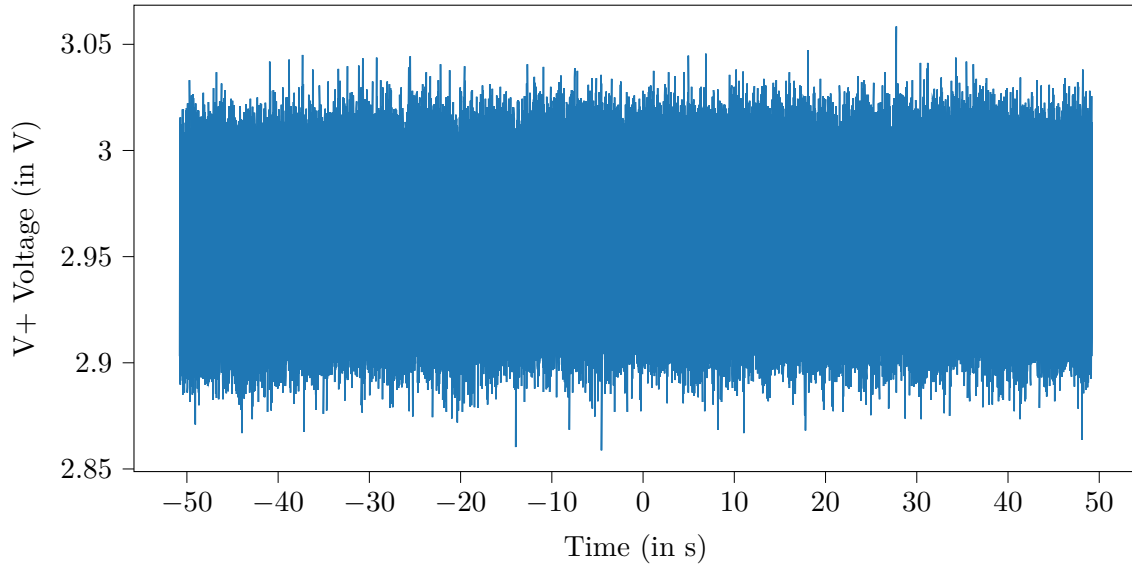


Figure 4.10.: Short term stability of $V+$ as delivered by the Keysight 34972A DAC (ch. 204); measured with Tektronix MSO64

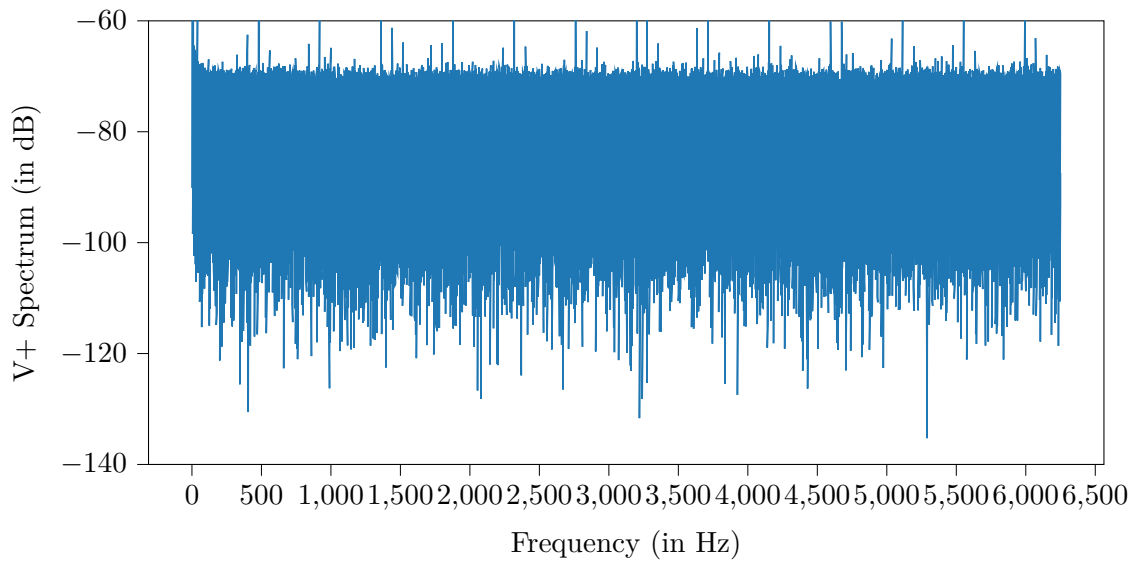


Figure 4.11.: Power spectrum of $V+$

4.5.5.4. Conclusion

The short term noise with $\sigma_{V,+,\text{shortterm}} = 50 \text{ mV}$ is fairly high compared to the other DAC channel (with a higher output voltage). But these variations are not visible on the multimeter due to the lower bandwidth ($\sigma_{V,+,\text{longterm}} = 0.154 \text{ mV}$). This suggests the power supply can simply be stabilized with a RC lowpass or just a capacitor at the devices supply voltage input.

But even without compensation the effects of the high frequency noise could not be seen in the attenuation, so device naturally rejects high frequency noise on its supply input.

4.5.6. Stability requirements of the case temperature θ_{case}

4.5.6.1. Required stability

To asses acceptable temperature change, first the influence of the device temperature of the attenuation is measured. For that the bottom of the device is fixed to a rectangular iron profile with zip ties. The iron profile is heated with the tip of a soldering iron (set to 150°C) for 1 min and then allowed to cool for 20 min. This cycle is repeated three times and the device temperature and the attenuation are measured once every 2 s. Due to the dynamic flow of heat from the soldering iron to the iron profile and through device itself, a strong hysteresis is visible in the curve in Figure 4.12.

To linearly approximate the temperature influence, the single measurements are binned together for similar temperature values (rounded to two decimal places). Then a mean operation is applied over the binned values (see Figure 4.13).

From that the slope of the curve is taken at $\vartheta_{\text{case},0} = 23^\circ\text{C}$ ³.

With a slope of $\left. \frac{dA(\vartheta_{\text{case}})}{d\vartheta_{\text{case}}} \right|_0 = 0.0075 \frac{\text{dB}}{\text{K}}$, the influence on attenuation becomes

$$\Delta A(\vartheta_{\text{case}}) = \left. \frac{dA(V_{\text{control}})}{dV_{\text{control}}} \right|_0 \cdot \Delta T_{\text{case}} \quad (4.14)$$

$$\Delta A(\vartheta_{\text{case}}) = 0.0075 \frac{\text{dB}}{\text{K}} \cdot \Delta V + \quad (4.15)$$

which means the allowed deviation of ϑ_{case} from $\vartheta_{\text{case},0}$ becomes

$$|\Delta \vartheta_{\text{case}}| = |\Delta A(\vartheta_{\text{case}})| \cdot \left| \left[\left. \frac{dA(\vartheta_{\text{case}})}{d\vartheta_{\text{case}}} \right|_0 \right]^{-1} \right| \quad (4.16)$$

$$= 0.005 \text{ dB} \cdot 133.33 \frac{\text{K}}{\text{dB}} = 0.666 \text{ K} \quad (4.17)$$

This would even be hard to achieve in climatized office spaces (like the IBPT RF lab), since aird conditioners can only keep the room temperature stable to about 2°C (depending on the distance to the air outlet, other heat sources in the room, open windows, etc.).

³This is not necessarily room temperature or expected operating temperature of the device but a convenient choice to get a linear curve section.

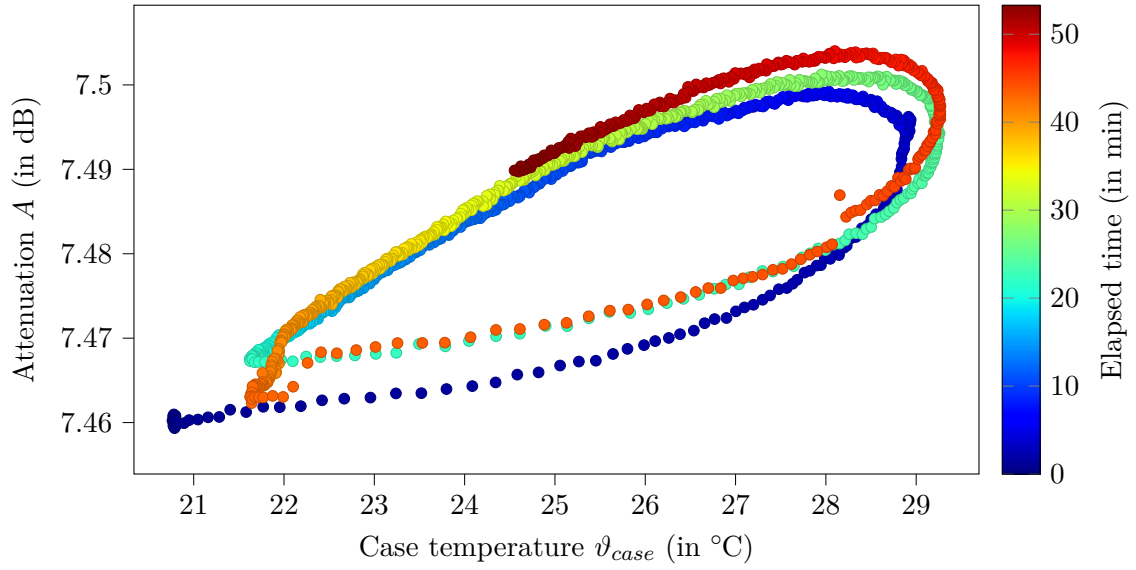


Figure 4.12.: Attenuation over case temperature; color scale shows time progress of the total measurement

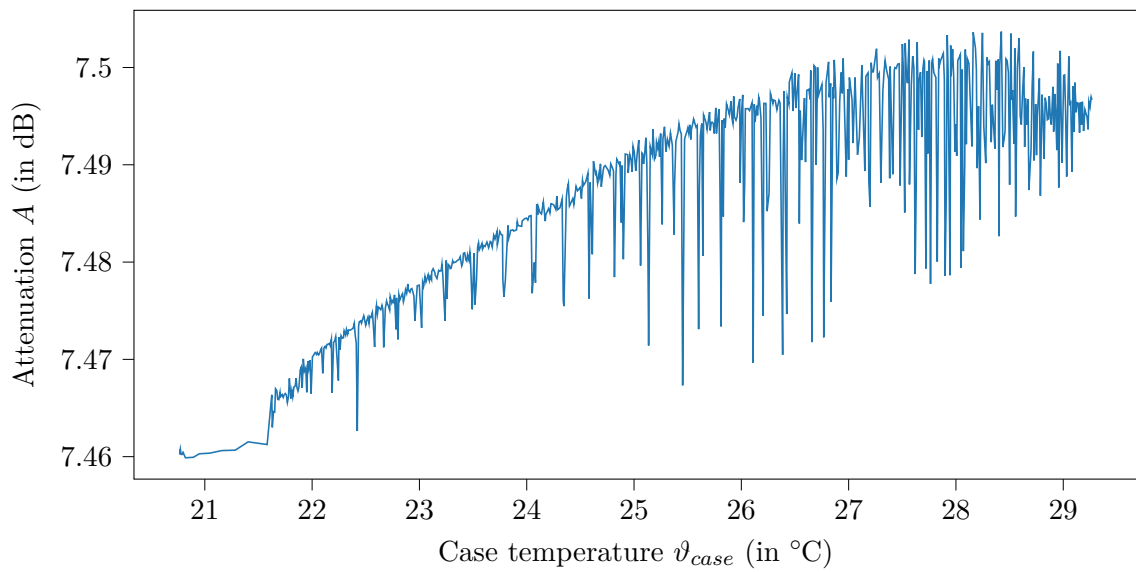


Figure 4.13.: Attenuation over case temperature

4.5.6.2. Conclusion

The results in Figure 4.13 and Equation 4.16 suggest two solutions:

- Either mount the device in a temperature controlled cabinet to keep the temperature constant.
- Or since the plot in Figure 4.13 shows the slope becoming more flat towards higher temperatures, it could may be possible to operate the device on purpose at higher case temperatures (According to the data sheet[3], the maximum operating temperature is 85 °C).

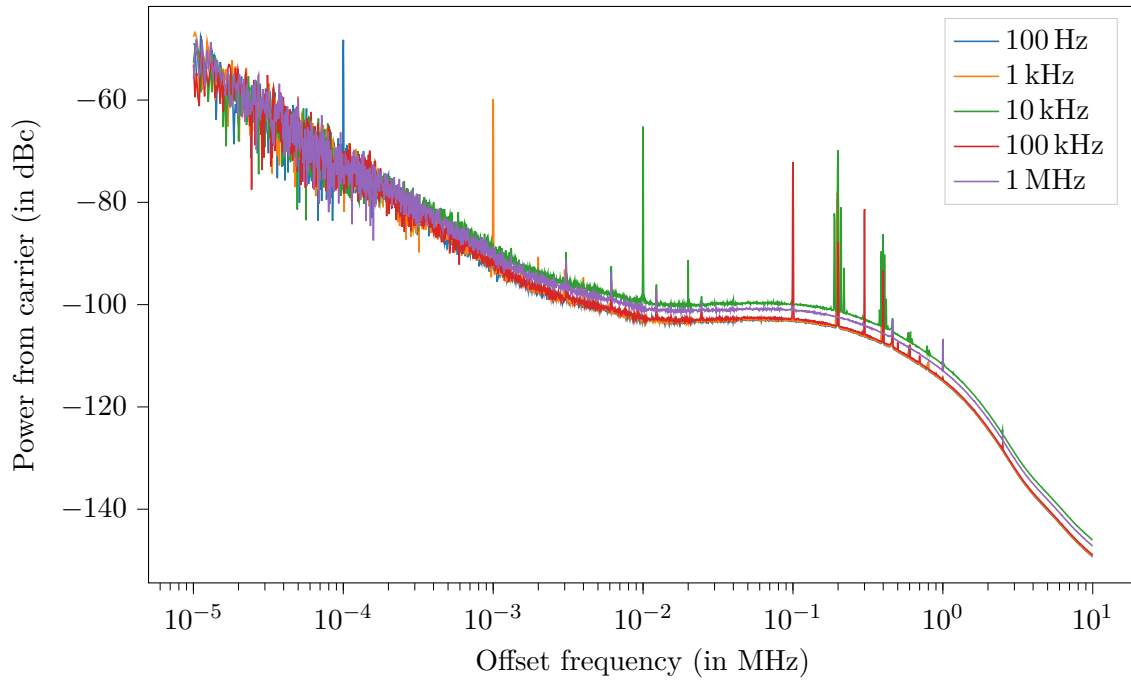


Figure 4.14.: Spectrum (measured with Holzworth HA7062A (subsubsection A.7.1)) showing the effect of modulating $V_{control}$ with different frequencies (Modulation amplitude: 1 V)

4.5.7. $V_{control}$ Frequency response

Using a non inverting adder with a *TS912IN* operational amplifier, a sine wave with constant offset is made, which is then used to drive the control voltage $V_{control}$. The result for different sine wave frequencies is shown in Figure 4.14.

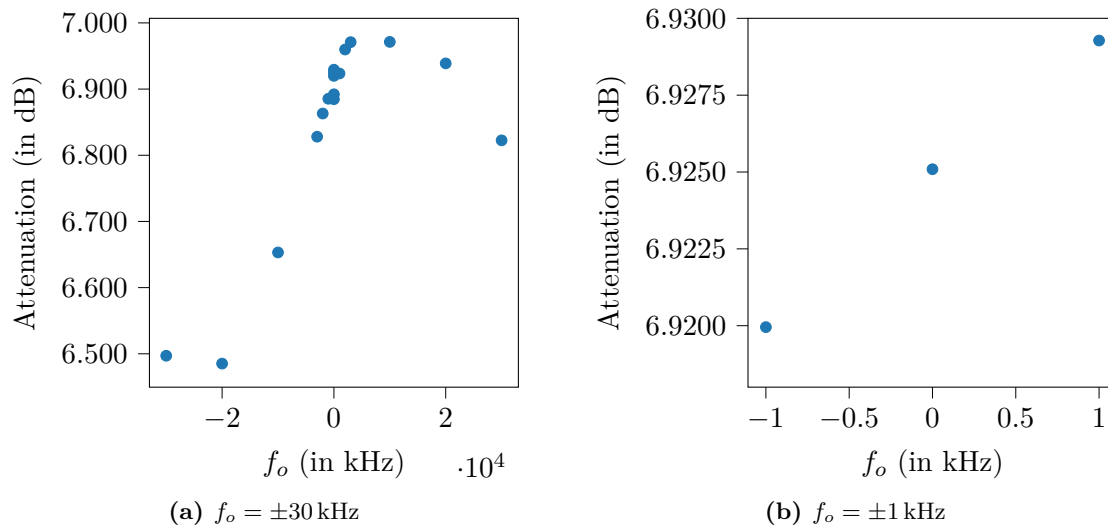


Figure 4.15.: Attenuation vs. offset frequency $f_o = f - 3 \text{ GHz}$

4.5.8. Influence of RF frequency variations

In this section the influence of a varying RF frequency on attenuation is examined. For that the set frequency of the R&S SMC100 signal generator is varied while the attenuation is measured with the HP E4419B RF power meter. The result is shown in Figure 4.15.

4.5.9. Testing the Attenuator in the RF cabinet at FLUTE

Without FLUTE being switched on, the attenuator is left in the RF cabinet in the bunker basement. Over the course of 100 h, the case temperature is taken every two seconds and the deviation from the mean temperature 25.4°C is computed (see Figure 4.16). The figure also shows a power spectrum (calculated using Welch's method with a hanning window) of the temperature deviation.

With a standard deviation of 0.05522 K , a maximum positive swing of 0.18 K and a maximum negative swing of 0.17 K (a span of 0.3559 K), the temperature stability is well inside the 0.6 K tolerance.

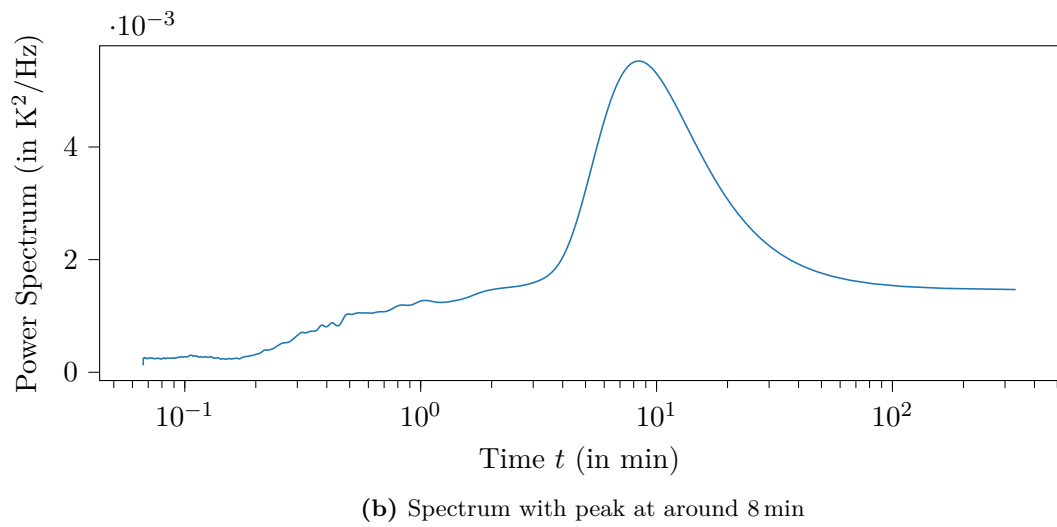
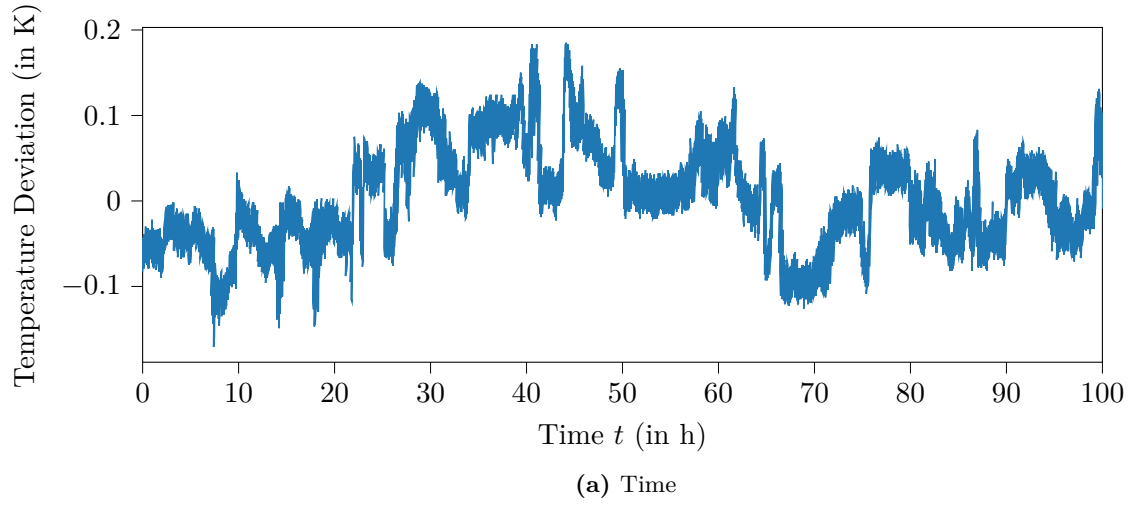


Figure 4.16.: Temperature of the attenuator inside the RF cabinet without a load

4.6. Implementing control algorithm

5. Results

6. Conclusion and Outlook

6.1. Conclusion

6.2. Outlook

Appendix

A. Lab Test and Measurement Equipment

A.1. Benchtop multimeters

A.1.1. Agilent 34411A

Table A.1.: Agilent 34411A specifications

Specification	Value
	DC volt
Digits	6 1/2
Measurement method	cont integrating multi-slope IV A/D converter
Accuracy (10 V range, 24 hours)	0.0015 % + 0.0004 % (% of reading + % of range)
Bandwidth	15 kHz (typ.)

Table A.2.: Agilent 34411A some SCPI commands

Description	Example command	Example return
Read current measurement	READ?	+2.84829881E+00 (2.848 V)

A.1.2. Keysight 34470A

Table A.3.: Keysight 34470A specifications

Specification	Value
	DC volt
Digits	7 1/2
Measurement method	cont integrating multi-slope IV A/D converter
Accuracy (10 V range, 24 hours)	0.0008 % + 0.0002 % (% of reading + % of range)
Bandwidth (10 V range)	15 kHz (typ.)

Table A.4.: Keysight 34470A some SCPI commands

Description	Example command	Example return
Read current measurement	READ?	+9.99710196E+00 (9.997 V)

A.2. Data Acquisition/Switch Unit

A.2.1. Keysight 34972A

Table A.5.: Keysight 34972A specifications

Specification	Value
	34907A (Multifunction module)
DAC range	± 12 V
DAC resolution	16 bit ($2^4 \text{ V} / 2^{16} = 366.21 \mu\text{V}$ per bit)
DAC maximum current	10 mA
	34901A (20 channel multiplexer)

Table A.6.: Keysight 34972A some SCPI commands

Description	Example command	Example return
Read current measurement	READ?	+2.00200000E+01 (20.02 °C)
Set DAC voltage of ch 204 to 3.1 V	SOUR:VOLT 3.1, (@204)	

A.3. Oscilloscopes

A.3.1. Tektronix MSO64

Table A.7.: Tektronix MSO64 specifications

Specification	Value
Bandwidth	6 GHz
Sample rate	25 GS/s
ADC resolution	12 bit
DC gain accuracy (@ 50 Ω , >2 mV/div)	± 2 %

Table A.8.: Tektronix MSO64 some SCPI commands

Description	Example command	Example return
Read mean of measurement 1 (current acq.)	MEASUREMENT:MEAS1:RESULTS:CURR:MEAN?	3.0685821787408

A.4. RF signal generator

A.4.1. Rohde and Schwarz SMC100A

Table A.9.: Rohde and Schwarz SMC100A specifications

Specification	Value
Frequency range	9 kHz to 3.2 GHz
Maximum power level	17 dBm
SSB phase noise (@ 1 GHz, $f_o = 20$ kHz, $BW = 1$ Hz)	-111 dBc
Level error	<0.9 dB

Table A.10.: Rohde and Schwarz SMC100A some SCPI commands

Description	Example command	Example return
Set RF power level to 10.5 dBm	SOUR:POW 10.5	
Set RF frequency to 3.1 GHz	SOUR:FREQ:FIX 3.1e9	
Enable the RF output	OUTP on	

A.5. RF power meter

A.5.1. HP E4419B

Table A.11.: HP E4419B specifications

Specification	Value
Digits	4
Accuracy (abs. without power sensor)	± 0.02 dB
Power probe: E4412A	
Frequency range	10 MHz to 18 GHz
Power range	−70 dBm to 20 dBm

Table A.12.: HP E4419B some SCPI commands

Description	Example command	Example return
Measure power on input 1	MEAS1?	+2.89435802E+000 (2.894 dBm)

A.6. Vector Network Analyzer

A.6.1. Agilent E5071C

Table A.13.: Agilent E5071C specifications

Specification	Value
Frequency range	9 kHz to 8.5 GHz

A.7. Phase noise analyzer

A.7.1. Holzworth HA7062C

Table A.14.: Holzworth HA7062C specifications

Specification	Value
DUT input frequency	10 MHz to 6 GHz
Measurement bandwidth	0.1 Hz to 40 MHz offsets

Bibliography

- [1] RadiaBeam, *Faraday Cups*. [Online]. Available: http://www.radiabeam.com/upload/catalog/pdf/14272334342015-03-24_faraday-cups.pdf.
- [2] P. Synotech, *PCB 421A25 Charge Amplifier*.
- [3] Mini-Circuits, *ZX73-2500+ Voltage Variable Attenuator*.
- [4] R. W. Waugh, "A Low-Cost Surface Mount PIN Diode π Attenuator", vol. 35, no. 5, pp. 280–284, 1992.